UC Davis
UC Davis Previously Published Works

Title

Peripheral Blood Transcript Signatures after Internal 131I-mIBG Therapy in Relapsed and Refractory Neuroblastoma Patients Identifies Early and Late Biomarkers of Internal 131I Exposures

Permalink

https://escholarship.org/uc/item/12b067vm

Journal

Radiation Research, 197(2)

ISSN

0033-7587

Authors

Evans, Angela C
Setzkorn, Tim
Edmondson, David A
et al.

Publication Date

2022-02-01

DOI

10.1667/rade-20-00173.1

Peer reviewed

Peripheral Blood Transcript Signatures after Internal ^{131}I-mIBG Therapy in Relapsed and Refractory Neuroblastoma Patients Identifies Early and Late Biomarkers of Internal [131]I Exposures

Angela C. Evans[a,b,1], Tim Setzkorn[c], David A. Edmondson[d], Haley Segelke[b], Paul F. Wilson[a], Katherine K. Matthay[e], M. Meaghan Granger[f], Araz Marachelian[g], Daphne A. Haas-Kogan[h], Steven G. DuBois[i], Matthew A. Coleman[a,b,2]

[a]Department of Radiation Oncology, University of California Davis, Sacramento, California;

[b]Lawrence Livermore National Laboratory, Livermore, California;

[c]Technical University of Munich, School of Medicine, Germany;

[d]Cincinnati Children's Hospital Medical Center, Cincinnati, Ohio;

[e]Department of Pediatrics, University of California San Francisco School of Medicine, San Francisco California;

[f]Department of Pediatrics, Cook Children's Hospital, Fort Worth, Texas;

[g]Department of Pediatrics, Children's Hospital Los Angeles, Los Angeles, California;

[h]Department of Radiation Oncology, Brigham and Women's Hospital and Dana-Farber Cancer Institute, Boston, Massachusetts;

[i]Dana-Farber/Boston Children's Cancer and Blood Disorders Center, Boston, Massachusetts

Abstract

^{131}I-metaiodobenzylguanidine (^{131}I-mIBG) is a targeted radiation therapy developed for the treatment of advanced neuroblastoma. We have previously shown that this patient cohort can be used to predict absorbed dose associated with early ^{131}I exposure, 72 h after treatment. We now expand these studies to identify gene expression differences associated with ^{131}I-mIBG exposure 15 days after treatment. Total RNA from peripheral blood lymphocytes was isolated from 288 whole blood samples representing 59 relapsed or refractory neuroblastoma patients before and after ^{131}I-mIBG treatment. We found that several transcripts predictive of early exposure returned to baseline levels by day 15, however, selected transcripts did not return to baseline. At 72 h, all 17 selected pathway-specific transcripts were differentially expressed. Transcripts *CDKN1A* ($P < 0.000001$), *FDXR* ($P < 0.000001$), *DDB2* ($P < 0.000001$), and *BBC3* ($P < 0.000001$) showed the highest up-regulation at 72 h after ^{131}I-mIBG exposure, with mean $\log_2$ fold changes of 2.55, 2.93, 1.86 and 1.85, respectively. At day 15 after ^{131}I-mIBG, 11 of the 17 selected transcripts were differentially expressed, with *XPC*, *STAT5B*, *PRKDC*, *MDM2*, *POLH*, *IGF1R*, and *SGK1* displaying significant up-regulation at 72 h and significant down-regulation at day 15.

[2]Address for correspondence: Department of Radiation Oncology, University of California Davis, Sacramento, CA; coleman16@llnl.gov.
[1]Scholar-in-Training.

Interestingly, transcripts *FDXR* ($P = 0.01$), *DDB2* ($P = 0.03$), *BCL2* ($P = 0.003$), and *SESN1* ($P < 0.0003$) maintained differential expression 15 days after ^{131}I-mIBG treatment. These results suggest that transcript levels for DNA repair, apoptosis, and ionizing radiation-induced cellular stress are still changing by 15 days after ^{131}I-mIBG treatment. Our studies showcase the use of biodosimetry gene expression panels as predictive biomarkers following early (72 h) and late (15 days) internal ^{131}I exposure. Our findings also demonstrate the utility of our transcript panel to differentiate exposed from non-exposed individuals up to 15 days after exposure from internal [131]I.

Editor's note.

The online version of this article (DOI: https://doi.org/10.1667/RADE-20-00173.1) contains supplementary information that is available to all authorized users.

INTRODUCTION

Biodosimetry assays are employed as surrogate measurements or supplements to physical ionizing radiation dosimetry that are based on assaying the outcomes of cellular DNA damage responses (DDR) after unanticipated radiation exposures (1). Much progress has been made to increase the sensitivity and throughput of various types of biodosimetry assays (2), with the intent that in the event of large-scale radiation incidents, these techniques will allow triaging of exposed individuals so that those with higher likelihood of severe radiation damage can be urgently treated (3). In addition, these assays can provide more refined estimates of true physical doses received by exposed individuals.

There are several physical methods to estimate radiation dose including radiographic film, thermoluminescent dosimetry, optically stimulated luminescence (OSL) dosimetry, and electron paramagnetic resonance (EPR) measurements of teeth (4–6). While these external dosimetry methods may prove useful, they present multiple challenges including issues of sensitivity and concerns over partial-body irradiation scenarios. Furthermore, OSL exposure estimates rapidly degrade when exposed to ambient light (4, 5), and EPR analysis is based on a local, rather than a whole-body absorbed dose (6). Therefore, additional biological markers that also accurately predict absorbed dose over time postirradiation are still needed (2, 7–10).

While the dicentric chromosome assay has traditionally been utilized as the "gold standard" to estimate absorbed dose by measuring dicentric chromosome numbers per cell in mitogen-stimulated peripheral blood lymphocytes, and more recently as a measurement of DNA double-strand break associated nuclear foci (e.g., g-H2AX pS139, 53BP1) levels after irradiation, it is not readily scalable and is time intensive (11). Gene expression analysis, on the other hand, is a robust and well-validated technique that can be quite feasible for screening a large cohort of affected individuals in the case of a disaster scenario, as it can be readily scaled-up and has a rapid turnaround. Thus, recent developments in gene expression profiling have shown that this technique may be a suitable alternative as well as supplement to both physical dosimetry and cytogenetic assays, as it can serve to estimate both whole- and partial-body radiation doses in both human and mouse models (12–16).

In addition to being less labor intensive, quantitative real-time PCR or microarray-based analyses have shown many biological pathways and genes of interest are modulated in response to radiation (2, 17), and several highly predictive mRNA and miRNA transcripts have been identified that are predictive of dose in human derived samples (8, 10, 14). These studies have proven useful for establishing panels of gene transcripts with increased sensitivity that are rapidly deployable and scalable for application in a disaster scenario.

While most radiation gene expression studies have been focused only on external irradiation scenarios, several groups have recently developed internal radiation exposure models with an emphasis on mouse-based studies (13, 15, 16, 18). Previous gene expression analyses for internal radiation exposures in humans have typically focused on biomarkers of multiple organ damage (19–21), but these did not look for DDR-related signatures in the peripheral blood as a readily available source of biodosimetry markers. More recently, DDR-related signatures in the peripheral blood have been studied in prostate cancer patients undergoing targeted radiation therapy (22). In addition, DDR-related signatures in peripheral blood lymphocytes have been seen shortly after patients undergo low-dose treatments for neurological procedures (23, 24).

Previous work on internal exposures to ^{131}I-metaiodobenzylguanidine (^{131}I-mIBG), a commonly used targeted radiotherapeutic for advanced neuroblastoma (25, 26), has demonstrated the utility of using well known transcripts for biodosimetry amongst DNA repair and apoptosis pathways. We have previously shown that these same transcripts can be applied in chemoradiotherapy patients as a model system for characterizing internal ^{131}I radiation exposures (27, 28). In brief, Edmondson et al. characterized the dosimetry of ^{131}I using a three-compartment model in a pilot study of high-risk neuroblastoma patients treated with ^{131}I-mIBG. In that study, an exponential decay curve of ^{131}I activity was measured through a radiation detector that was situated above the patient. We utilized our experimentally derived decay constants from our time-activity curve to estimate total cumulative activity and ultimately mean absorbed dose in these patients. We then performed multiple regression analysis and attained a mathematical equation to estimate gene-expression based dose prediction with time. In short, Edmondson et al. (28) demonstrated that transcripts known to be affected by external irradiation are likewise good indicators of internal radiation exposures at 72 and 96 h after ^{131}I-mIBG treatment. Campbell et al. (27) also showed that transcripts measured in the peripheral blood at 72 h may be predictive of treatment toxicities in relapsed and refractory neuroblastoma patients (27). Extending these findings to later time points may enhance the utility of radiation-specific gene expression panels to correlate biomarkers of patient response to total absorbed dose based on treatment with ^{131}I-mIBG, as well as identify additional biomarkers that may be predictive of sub-acute toxicities. These transcript panels may also be used as an efficient tool to triage whole- and partial-body irradiated individuals after an unanticipated radiation or nuclear incident.

The current study investigates ^{131}I-mIBG therapy-induced gene expression changes in pediatric relapsed and refractory neuroblastoma patients at both 72 h and 15 days after exposure. The goal of this study was to further characterize our established radiation-responsive transcripts and evaluate their differential expressions at both 72 h and 15 days

after ^{131}I-mIBG treatment, as compared to untreated baseline samples. To our knowledge, this is the first demonstration of isolating whole blood at 15 days after ^{131}I-mIBG treatment in humans for validating transcripts known to be responsive to both internal and external irradiation and calculating expression differences in patient peripheral blood. We also demonstrate that our selected transcript panel differentiates between exposed and non-exposed samples 15 days after ^{131}I-mIBG treatment. These findings expand upon our previous studies investigating the biological responses to ^{131}I-mIBG in pediatric neuroblastoma patients and may potentially be extended to predict biomarkers of systemic total-body exposures up to 2 weeks after a radiation incident involving internalized isotopes.

MATERIALS AND METHODS

Clinical Trial Patient Recruitment and mIBG Study

The NANT11-01 trial was a randomized phase II trial comparing response rates in patients with relapsed/refractory mIBG-avid neuroblastoma treated with ^{131}I-mIBG therapy alone, ^{131}I-mIBG with vorinostat (SAHA), or ^{131}I-mIBG with both vincristine and irinotecan (ClinicalTrials.gov identifier: NCT02035137). These patients were selected based on several inclusion as well as exclusion criteria as outlined on clinical trials.gov website (ClinicalTrials.gov identifier: NCT02035137). All 59 patients in this study were treated with ^{131}I-mIBG 18 mCi/kg [6.66×10^8 Bq/kg] (maximum absolute dose 1,200 mCi [4.44×10^{10} Bq]) intravenously over 90–120 min and received proper thyroid blockade and bladder protection using potassium iodide (6 mg/kg loading dose then 1 mg/kg/dose every 4 h on days 1–7 and then 1 mg/kg/dose once daily on days 8–43), and a Foley catheter as previously described (29). NANT11-01 included an optional correlative study to evaluate biomarkers of radiation exposure. Patients (or legal guardians for minor subjects) included in the current analysis provided consent for the parent trial and opted in for these gene expression studies. The Institutional Review Board of participating trial sites, as well as the University of California Davis and Lawrence Livermore National Laboratory, approved this study.

Blood Sample Processing

Peripheral blood was drawn using PAXgene RNA blood tubes (Qiagen) in two separate samples prior to ^{131}I-mIBG treatment (Baseline A and Baseline B) as well as a sample at 72 h and day 15 after ^{131}I-mIBG exposure (treated). Baseline A was obtained prior to any protocol therapy for all patients. Baseline B for patients on the mIBG only arm was drawn 1–2 days later and reflects no intervening therapy. Baseline B for patients on the other arms of the trial that contain additional putative radiation sensitizers (vorinostat or vincristine/irinotecan) was drawn 1–2 days after Baseline A and reflects the intervening radiation sensitizer therapy but not the effect of mIBG (Fig. 1). Once ^{131}I-mIBG is administered, this is day 1, and the 72 h or day 15 blood draw occurs either 3 days or 15 days after ^{131}I-mIBG treatment. Blood tubes were stored at −80°C for several weeks postirradiation and before blood processing began, ensuring that the levels of ^{131}I had sufficiently decayed prior to analysis. Total RNA was then extracted using MagMAX™ for Stabilized Blood Tubes RNA Isolation Kit, compatible with PAXgene RNA tubes (Invitrogen) following the manufacturer's instructions. RNA was eluted in 50 μL aliquots and stored at −80°C for

later use. RNA was quantified via the NanoDrope One[C] spectrophotometer (Invitrogen) and Qubit 3.0 Fluorometer (Invitrogen). Total RNA was isolated and prepared for cDNA synthesis prior to quantitative real-time PCR (qPCR) analysis. In total, 288 blood samples were processed for this study. Each patient serves as his or her own control for differential analysis.

Biodosimetry Transcript Selection

Previously published radiation-responsive transcripts were selected for validation within our current study (8, 30–33) and are shown in Table 1. The GAPDH housekeeping gene was selected for normalization based on our previous findings using multiple housekeeping transcripts in Edmondson et al. (28). Most transcripts of interest were downstream effectors of the tumor suppressor protein 53 (TP53 or p53) pathway. Additional transcripts were associated with pathways involved in cellular stress as well as TP53 DNA damage response (Table 1).

cDNA Synthesis

In preparation for quantitative real-time PCR (qPCR), 200 ng of RNA was converted to cDNA via the High-Capacity RNA-to-cDNA kit (Applied Biosystems). If RNA was too dilute, it was concentrated via Speedvac 2.0 (Savant, DNA SpeedVac 120) prior to cDNA synthesis. The cDNA synthesis reactions incubated in a thermocycler at 37°C for 60 min, 95°C for 5 min, and then held at 4°C. Once complete, the cDNA was pre-amplified with Taqman[™] PreAmp Master Mix (Applied Biosystems). A custom pooled assay mix of TaqMan primers, including all 18 transcripts for this study, were combined along with the cDNA template and the Taqman[™] PreAmp master mix. Reactions pre-amplified at 95°C for 10 min, followed by 14 cycles of (95°C for 15 s, 60°C for 4 min) in a thermocycler. After pre-amplification, reactions were diluted 20-fold in 1X TE buffer and stored at −15°C to −25°C in preparation for qPCR.

Quantitative Real-Time PCR (qPCR)

Quantitative real-time PCR was used to analyze the transcript expression level differences for each patient at each exposure time point. Each reaction used 5x TUFF TAQ QPCR Master Mix+Rox (Rebel Bioscience, Portland, OR), TaqMan[™] primers (Table 1), pre-amplified cDNA, and nuclease-free water for a total volume of 25 µL per reaction. Each transcript was analyzed in triplicate. Reactions were placed in a 7900HT Fast Real-Time PCR machine (Applied Biosystems). The following parameters were used: 95°C for 10 min, followed by 40 cycles of (95°C for 15 s, 60°C for 1 min). The cycle threshold (Ct) values from the qPCR curves were extracted at the logarithmic growth phase of the curve. The delta-delta Ct methods was used to calculate the fold changes ($2^{-\Delta\Delta Ct}$), as previously described (28). The $\log_2$ of the linear fold changes was calculated for comparisons.

Statistics and Analysis

For qPCR, the $2^{-\Delta\Delta Ct}$ was used to calculate the fold change, as previously published (28). A *P* value of 0.05 was used as a cutoff to determine statistical significance. *P* values are labeled as <0.05 (*), <0.01 (**), <0.001 (***), and <0.0001 (****) throughout the article.

At 72 h and day 15 after ^{131}I-mIBG, patient fold changes were calculated with respect to Baseline A (untreated) expression levels across all patient sets. Each baseline sample was analyzed in the same manner as the exposed samples. Fold changes between Baseline B and Baseline A samples account for either normal variability in the baseline data (^{131}I-mIBG only group) or the effects of the additional drug(s) (vorinostat or vincristine/irinotecan patients) prior to radiation exposure. The "Baseline" fold changes (Baseline B vs. Baseline A) were then used for comparisons with later time points. Thus, any variability under the "Baseline" fold change will account for the potential effect(s) of the radiation sensitizers when comparing to fold changes at 72 h or 15 days after ^{131}I-mIBG treatment. The $\log_2$ of the linear fold changes were calculated and multiple t tests were performed to determine significance between various time points. Data plotting and t tests used GraphPad software.

Calculated kinetic model (Km) doses at 72 h were determined based on absolute mCi of ^{131}I-mIBG received and fitted to the linear decay curve as previously described (28). A linear regression model was then derived using the top priority transcript fold changes to generate a gene expression-based dose (GE) as previously described (28). Predicted doses for 32 random samples (16 at 72 h and 16 unexposed) were fit using our newly derived gene expression based linear regression model (Table 2), along with prediction intervals (PI) and confidence intervals (CI).

Partial Least Squares Discriminant Analysis

As a preliminary assessment for how strongly $\log_2$ transformed transcripts can predict whether a patient has been exposed (72 h or 15 days after treatment) from unexposed patients (prior to treatment), we used partial-least squares discriminant analysis (PLS-DA). PLS-DA is a linear classification model generated from data that can be used to classify new samples. PLS-DA was applied using only the top 7 transcripts (*CDKN1A*, *FDXR*, *BAX*, *BCL2*, *BCL2L1*, *DDB2* and *PRKDC*) at 72 h, and two PLS-DA runs were applied to 15-day samples (top 7 transcripts and all transcripts). We assessed generalizability of the model by performing leave-one-out cross-validation. We calculated sensitivity, specificity, and area under the curve (AUC) as measures of model performance. Implementation of PLS-DA was done using the R package mixOmics (34).

RESULTS

Patient and Sample Characteristics

Fifty-nine pediatric patients with relapsed or refractory neuroblastoma provided samples for the current analysis (Fig. 1). There were 25 males and 34 females included in this analysis. The ages of the patients range from 1–26, with a mean age of 7. There were 22 of the 59 patients that received two rounds of ^{131}I-mIBG treatment (four ^{131}I-mIBG alone, nine ^{131}I-mIBG+vincristine/irinotecan patients, and nine ^{131}I-mIBG + vorinostat patients), and we received samples from only a second course of treatment from one patient (^{131}I-mIBG + vincristine/irinotecan). We confirmed with this dataset our previous findings that our gene expression transcript panel was not statistically different after the second course of treatment compared to the first course of treatment [Supplementary Fig. S1; https://doi.org/10.1667/RADE-20-00173.1.S1; (28)]. Thus, individuals who had a previous course of treatment

were analyzed independently of their second course of treatment. Altogether, there were 81 patient sets (courses of treatment) in this study (20 ^{131}I-mIBG only, 31 ^{131}I-mIBG + vincristine/irinotecan, and 30 ^{131}I-mIBG + vorinostat). One patient set did not have a 72-h time point and only had baseline and 15-day blood draws. In total, there were 80 patient sets with a 72-h time point (57 patient sets from Course 1 and 23 patient sets from Course 2, with one patient set only having received Course 2 samples) and 16 patient sets at the 15-day time point (12 patient sets from Course 1 and 4 patient sets from Course 2, with one patient set only having received Course 2 samples). Transcripts *GAPDH*, *CDKN1A*, *FDXR*, *BAX*, *BCL2*, *BCL2L1*, *DDB2*, and *PRKDC* were considered our top priority transcripts and were analyzed with all 58 patients (n = 80 courses of treatment) at 72 h and all 13 patients (n = 16 courses of treatment) at day 15. Second priority transcripts *GADD45A*, *XPC*, *STAT5B*, *SESN1*, *POLH*, *BBC3*, *PCNA*, *IGF1R*, and *SGK1* comprised of 12 patients (n = 14 courses of treatment) at day 15 or 26 patients (n=31 courses of treatment) at 72 h. *MDM2* was added to the transcript panel after many samples had already been analyzed and comprised of 12 patients (n = 14 courses of treatment) at day 15 or 11 patients (n = 13 courses of treatment) at 72 h. The total number of patients, total courses of treatment, *P* values, and FDR values for all transcripts at both 72 h and day 15 as compared to untreated controls are summarized in Supplementary Table S1 (https://doi.org/10.1667/RADE-20-00173.1.S1). RNA yield varied between 4.7 and 574 ng/μl, with average A260/280 absorbance values of 2.2, and A260/230 absorbance values of 0.9 across all samples. The mean RIN value collected was 8. Our analysis focused on differentially expressed transcripts within these patient sets for comparing early (72 h) and late (day 15) responses after ^{131}I-mIBG via quantitative real-time PCR (Table 1 and Fig. 1b).

[131]I-mIBG Exposure Alters Early Gene Expression Levels Compared to Baseline

Figure 2a shows the range of transcript fold changes at 72 h as compared to Baseline A samples. Overall, 17 transcripts demonstrated significant gene expression differences at 72 h as compared to baseline controls, with 14 transcripts displaying significant up-regulation and 3 transcripts demonstrating significant down-regulation (Fig. 2a and Supplementary Fig. S2a; https://doi.org/10.1667/RADE-20-00173.1.S1;). At 72 h after ^{131}I-mIBG treatment, the average $\log_2$ transformed fold changes across the transcript panel ranged from –1.786 (*BCL2L1*) to +2.930 (*FDXR*) across all 80 patient sets. Several transcripts demonstrated significant up-regulation, including *CDKN1A* ($P < 0.000001$), *FDXR* ($P < 0.000001$), *DDB2* ($P < 0.000001$), and BBC3 ($P < 0.000001$) (Fig. 2a and Supplementary Fig. S2a). *FDXR* showed the highest levels of up-regulation at 72 h, with the median linear fold change of 7.77, and peak linear fold change of 25.85. *BCLXL* was heavily down-regulated at 72 h, with median linear fold change of 0.277 (about 1.85-fold down-regulated) over baseline samples (untreated controls).

Multiple Transcripts are Differentially Expressed 15 Days after ^{131}I-mIBG Exposure

Similar to the early exposed samples, all transcripts selected were measurable in qPCR assays 15 days after ^{131}I-mIBG treatment and a Baseline B to Baseline A (untreated control) fold change comparison was used to negate potential confounding factors from the radiosensitizer(s) (Fig. 2b). Nine transcripts were significantly down-regulated at day 15 compared to untreated controls, including *BCL2* ($P = 0.002583$), *XPC* ($P = 0.028870$),

STAT5B (*P* = 0.007300), *MDM2* (*P* = 0.002145), *PRKDC* (*P* = 0.001428), *SESN1* (*P* = 0.000287), *IGF1R* (*P* = 0.0005), (*POLH* (*P* = 0.000746), and *SGK1* (*P* = 0.009254) (Fig. 2b and Supplementary Fig. S2b; https://doi.org/10.1667/RADE-20-00173.1.S1). *FDXR* and *DDB2* (*P* = 0.01 and 0.03, respectively) maintained significant up-regulation at day 15 after exposure. Additionally, *BCL2* and *SESN1* expression remained down-regulated at both 72 h and day 15 (Fig. 3). Interestingly, *STAT5B*, *XPC*, *MDM2*, *PRKDC*, *POLH*, *SGK1*, and *IGF1R* were significantly up-regulated at 72 h but were significantly down-regulated at day 15 (Fig. 3 and Supplementary Fig. S2a and b; https://doi.org/10.1667/RADE-20-00173.1.S1). Expression levels of six radiation-responsive transcripts at early time points (*CDKN1A*, *GADD45A*, *BCL2L1*, *BAX*, *BBC3* and *PCNA*) did not display any differential expression at day 15 as compared to untreated controls, indicating a return to baseline expression levels (Figs. 2b and 3).

Comparison between Early and Late Time Points Show Differences in Gene Expression

Given the differential gene expression changes between early (72 h) and late (day 15) time points compared to untreated controls, we next sought to compare differences between 72 h and 15 days independently. Here, the $\log_2$ fold changes at both time points were calculated with respect to untreated Baseline A. Fourteen transcripts demonstrated significant modulation between early and late time points after ^{131}I-mIBG treatment (Fig. 2c and Supplementary Fig. S2c; https://doi.org/10.1667/RADE-20-00173.1.S1). Fold changes for thirteen of the fourteen transcripts were up-egulated at 72 h after exposure, and subsequently down-regulated at day 15. The only transcript that displayed significant down-regulation at 72 h as compared to 15 days was *BCL2L1*, an anti-apoptotic marker (Fig. 2c and Supplementary Fig. S2c; https://doi.org/10.1667/RADE-20-00173.1.S1).

Gene Expression-Based Dose Prediction is Consistent at 72 h but Inconclusive at Day 15

We calculated absorbed doses for all 80 patient sets at 72 h using the three-compartment biokinetic model based on the ^{131}I decay curve, amount of injected ^{131}I-mIBG activity, and patient body weight as previously described (28). These doses were termed kinetic model (Km) doses. We then applied a linear regression model on a random pool of 32 patient sets (16 treated at 72 h and 16 untreated) to predict dose based on gene expression values. We focused only on the top 7 priority transcripts (*CDKN1A*, *FDXR*, *BAX*, *BCL2*, *BCL2L1*, *DDB2* and *PRKDC*) for our gene expression dose estimation to ensure that all patients contained full datasets. Predicted doses based on the gene expression (GE) model fall between 1.55–2.97 Gy, and calculated Km doses for these 16 treated samples fall within 2.3–2.88 Gy with an R^2 value of ~0.89, suggesting that a linear regression model remains robust for predicting dose values in subjects treated with ^{131}I-mIBG (Table 2). We then performed PLS-DA with Leave-One-Out Cross Validation (LOO-CV) using the same top 7 transcripts on all 160 samples at 72 h (80 treated and 80 untreated) to predict exposed from unexposed individuals. LOO-CV predicted exposed from unexposed samples with 98% specificity and 92.5% sensitivity (Table 3).

Because our previously published three-compartment model only encompassed data up to 120 h, we could not use this model to predict doses at day 15. Therefore, we used the amount of injected ^{131}I-mIBG activity (mCi) to calculate the absorbed dose at day

15 using Eqs. (1)–(3) from our previous pilot study (28) in an attempt to calculate dose based on gene expression at the 15-day time point. The resulting doses from the biokinetic model were termed "observed" doses. We then performed linear regression and LOO-CV to create a gene expression model that would be relevant at day 15. Using our newly derived 15-day gene expression-based model, we predicted total dose absorbed at day 15 as compared to the observed dose from the biokinetic model (data not shown). Predicted doses from the 15-day gene expression results ($\log_2$ fold change compared to Baseline A) were indistinguishable from the predicted dose using untreated baseline samples (Time 0; $\log_2$ fold change comparing Baseline B to Baseline A). This suggests that 15 days may be too late to retrieve an accurate gene-expression based dose estimation reading within the peripheral blood from internal [131]I.

Transcripts are Strongly Predictive of Exposure Status Out to 15 Days

Although accurate or absolute dose prediction was inconclusive at day 15, we next sought to investigate if our gene expression panel could distinguish radiation exposed from unexposed individuals at day 15. Thus, we generated a predictive two-component PLS-DA model using gene expression results from 16 patients sets (Fig. 4). We ran PLS-DA with LOO-CV on our top 7 priority transcripts and predicted exposed vs. unexposed samples with 87.5% specificity, 87.5% sensitivity and an R^2 value of ~0.9 (Fig. 4 and Table 4). All 16 exposed samples were correctly identified as exposed, and only 1 false positive sample was incorrectly predicted as exposed (Fig. 4). We also performed PLS-DA and LOO-CV on our complete 17 transcript panel and found it to be slightly more specific than our top 7 transcripts alone, with 94% specificity and 87.5% sensitivity (Supplementary Fig. S3: https://doi.org/10.1667/RADE-20-00173.1.S1; and Table 4).

DISCUSSION

This study demonstrates the utility of using biodosimetry gene expression panels established for external irradiation scenarios for internalized ^{131}I exposures (and may be generally applicable to other internal radioisotopes) over later time points. Importantly, the data are derived directly from pediatric patients, an under-represented population rarely included in radiation exposure studies. These data were also useful for detecting transcriptional differences between early (72 h) and late (day 15) time points after ^{131}I-mIBG treatment in human chemo-radiotherapeutic patients using known radiation-responsive gene transcripts. Furthermore, our findings demonstrate that this gene expression panel is useful for predicting exposed from unexposed individuals out to 15 days and could accurately triage the exposed population with as little as 7 selected transcripts. These data may be useful in the event of a large-scale disaster between 3 days and up to 2 weeks after an initial exposure, allowing clinical assistance and resources to funnel to those in need while reassuring the worried well.

Previous external and internal biodosimetry studies provided transcript analysis usually within 3 days of exposure (10, 12, 14, 27, 28). To our knowledge, our study is unique in that it demonstrates the strength of using peripheral blood as a biomarker of DNA damage-related responses to internal ^{131}I in humans up to 15 days after exposure, demonstrating

further utility for expression panels with common transcripts of interest. We chose our two time points of interest, 72 h and 15 days, because they align nicely with the treatment plan for these relapsed/refractory neuroblastoma patients. There are radiation safety concerns with obtaining blood samples prior to 72 h after ^{131}I-mIBG treatment. Thus, 72 h (3 days) serves as our early time point. The 15-day time point was chosen as patients are clinically treated with an autologous stem cell boost at that time.

We utilized an expanded panel of TP53, PI3K/AKT, and MAPK-regulated transcripts and found that certain predictors of early exposure did not overlap with the later time point of 15 days. These data demonstrate that at 72 h after exposure, *CDKN1A*, *GADD45A*, *BAX*, *BBC3*, *PCNA*, and *BCL2L1* were key indicators of internal ^{131}I exposure, however, transcript fluctuations were time-dependent and were not significant at the later time point as compared to untreated controls. This demonstrates that these transcripts may be useful as early biomarkers of more recent ^{131}I exposures that could likewise be relevant to other beta-emitting radioisotopes of concern such as ^{90}Sr and [137]Cs. We also identified four transcripts that continued to maintain consistent gene expression differences at both early (72 h) and late (day 15) points: *FDXR*, *DDB2*, *BCL2* and *SESN1*. These transcripts may serve as novel biomarkers useful for triaging those exposed at both early and late time points, especially in the event of a nuclear disaster, where it may not be feasible to triage the entire exposed population from the worried well within three days. We also found that *STAT5B*, *XPC*, *MDM2*, *PRKDC*, *POLH*, *SGK1*, and *IGF1R* were the only transcripts in this study to be significantly up-regulated at the early time point and significantly down-regulated at the late time point. This indicates that these transcripts may be more sensitive to small changes in relevant radiation-responsive cell cycle and DNA damage response pathways, such as those mediated by TP53. This may also indicate transcripts that are susceptible to long-term toxicities associated with treatment, such as immune modulation and hematopoietic stem cell depletion/dysfunction associated with ^{131}I-mIBG treatment at later time points. It should also be noted that gene expression levels continued to change at day 15 after treatment, as most transcripts had not returned to baseline levels.

Our biodosimetry panel focused on several TP53-regulated transcripts of interest that have been previously identified as responsive to early radiation exposures of 3 days (35). These results coincide with previous reports of ex vivo irradiated samples from human peripheral blood, validating *FDXR* and *CDKN1A* as important biomarkers of early exposure for both internal and external sources of radiation (14, 36). Other external irradiation studies of TP53-responsive genes included *DDB2* and *MDM2*, which were also significantly up-regulated upon early exposures (35, 37). Although previous studies have investigated *CDKN1A*, *FDXR*, *MDM2*, and *DDB2* as candidate up-regulated biomarkers of radiation exposure (30, 35, 36), our study expands upon these findings to validate these transcripts as biomarkers of internal ^{131}I exposure at early time points. Similar to what we have seen previously in neuroblastoma patients, *CDKN1A* and *MDM2* also displayed a time-dependent up-regulation at 72 h and decreased with later time points (28). Interestingly, our study identified *FDXR* and *DDB2* as biomarkers of both early and late exposures, maintaining consistent up-regulation at 72 h and day 15 as compared to untreated controls.

We found that at day 15 the fold changes of our transcript panel differed from those at 72 h. We identified nine transcripts significantly down-regulated at day 15 as compared to untreated controls, which may indicate a delayed recovery response of these genes to return to normal levels from the effects of internal ^{131}I-mIBG exposure. It is also possible that the biological effects of ^{131}I may still be contributing to these transcript fluctuations at day 15, as the physical half-life of ^{131}I is ~8 days and there is still ongoing exposure 15 days after treatment initiation. This finding that transcripts are still fluctuating after two weeks of exposure will need to be considered when triaging and treating individuals long after an irradiation incident.

Here, we suggest that many transcripts initially designated as early biomarkers of ionizing radiation exposure are no longer predictive biomarkers of exposure after 15 days. In contrast to transcripts that we identified that are indicative of early exposures, we found that *BCL2* and *SESN1* remained significantly downregulated at day 15, indicating that DDR and apoptotic pathways may still be dysregulated at later time points. These transcripts differ from the standard transcripts studied with early exposures and may be relevant and impactful biomarkers at late exposures after 15 days, where gene expression levels are still changing.

Among the essential features of this model system is the well-defined patient exposure history, where samples were collected at both early and late time points post-^{131}I-mIBG treatment. Moreover, each subject provided blood before and after exposure, so that each individual acts as his or her own control. Furthermore, we utilized robust qPCR assays that are used in exposure scenarios over an extensive amount of radiation studies (35) and that have been previously validated as an accurate and reproducible method for analyzing ^{131}I-mIBG patient samples (38). This model system is also ideal for detecting biomarkers of acute toxicity (27) and extrapolating absorbed dose estimates from ^{131}I-mIBG exposures (28).

Despite the quick and reliable detection methods of qPCR, there is still a need for larger gene expression studies to better understand the overall association between transcripts and physiological effects associated with exposure outcomes. Another limitation of qPCR is that it is directed towards a specific transcript panel of interest, and it is not feasible for analyzing thousands of genes at once. Thus, analyzing gene expression levels via qPCR in combination with additional studies, like microarray and sequencing, may complement these findings and validate new genes and pathways responding to both early and late ^{131}I-mIBG exposures.

Although human data are the most relevant in the case of a radiation exposure, there are confounding factors within this study that may alter the gene expression results as compared to the normal population. First, all the individuals within this study have been diagnosed with relapsed or refractory neuroblastoma and may have been previously exposed to chemotherapeutic agents and/or surgery. In addition, these data encompass exposure conditions from children treated with potassium iodide to block and protect the thyroid, as well as concomitant chemotherapy or radiation sensitizers, which may or may not contribute at some level to the differential expression observed in the peripheral blood. Furthermore, similar studies in adults are limited due to the nature of this disease. It is also worth noting that this study encompasses 81 different patient sets amongst 59 different people, since

many patients had two courses of treatment. The impact of the autologous stem cell boost may have been the reason for seeing transcriptional responses resetting prior to the next round of treatment.

In the case of a large-scale radiation incident, estimating the dose for exposed individuals will help triage those that need immediate attention to relay the proper medical treatment. It is known that the timing since exposure can have drastic influence on dose estimate and clinical patient care (5, 39). Therefore, expanding the gene panel of interest out to different time points remains a key variable in providing accurate and reliable dose-estimation and clinical assistance in the event of an exposure disaster. In summary, we have shown in a human peripheral blood model system that there are unique transcripts that are differentially expressed at both early and late time points after ^{131}I-mIBG treatment. We have also identified key biomarkers responding to internal ^{131}I-mIBG at both early (72 h) and late (day 15) time points. In addition, *FDXR*, *DDB2*, *BCL2*, and *SESN1* maintained consistent differential expression at both 72 h and day 15, indicating biomarkers that may remain useful in a triage incident 15 days after exposure.

Furthermore, the modulation in gene expression at the day 15 time point can still discriminate between exposed and non-exposed individuals using a selected gene transcript panel associated with DNA damage signaling, apoptosis, cell cycle progression, and cellular stress response pathways. We can also predict exposed from the non-exposed at day 15 after treatment with 87.5% or 94% specificity using the weightings from our top priority transcripts or our full transcript panel, respectively. It is worth noting that these data not only serve to model ^{131}I dosimetry or internal exposure, but may ultimately be shown to provide a measure of patient toxicity or tolerance in the treatment of high-risk neuroblastoma patients (27). In the future, it will be of interest to investigate additional genome scale data such as arrays and next generation sequencing to expand our biodosimetry panel of interest and identify both patient-specific and treatment-specific responses to ^{131}I-mIBG exposure, including its relevance as a measure of overall patient outcome.

Supplementary Material

Refer to Web version on PubMed Central for supplementary material.

ACKNOWLEDGMENTS

REFERENCES

1. Levinson HS, Garber EB. Release of inorganic phosphate from irradiated yeast: radiation biodosimetry and evaluation of radio-protective compounds. Appl Microbiol. 1967; 15(2):431–40. [PubMed: 6029839]

2. Sproull M, Camphausen K. State-of-the-art advances in radiation biodosimetry for mass casualty events involving radiation exposure. Radiat Res. 2016; 186(5):423–35. [PubMed: 27710702]

3. Dainiak N, Waselenko JK, Armitage JO, MacVittie TJ, Farese AM. The hematologist and radiation casualties. Hematology Am Soc Hematol Educ Program. 2003:473–96. [PubMed: 14633795]

4. Sholom S, Dewitt R, Simon SL, Bouville A, McKeever SW. Emergency dose estimation using optically stimulated luminescence from human tooth enamel. Radiat Meas. 2011; 46(9):778–82. [PubMed: 21949479]

5. Swartz HM, Williams BB, Flood AB. Overview of the principles and practice of biodosimetry. Radiat Environ Biophys. 2014; 53(2):221–32. [PubMed: 24519326]

6. Trompier F, Burbidge C, Bassinet C, Baumann M, Bortolin E, De Angelis C, et al. Overview of physical dosimetry methods for triage application integrated in the new European network RENEB. Int J Radiat Biol. 2017; 93(1):65–74. [PubMed: 27584947]

7. Amundson SA, Bittner M, Chen Y, Trent J, Meltzer P, Fornace AJ Jr. Fluorescent cDNA microarray hybridization reveals complexity and heterogeneity of cellular genotoxic stress responses. Oncogene. 1999; 18(24):3666–72. [PubMed: 10380890]

8. Budworth H, Snijders AM, Marchetti F, Mannion B, Bhatnagar S, Kwoh E, et al. DNA repair and cell cycle biomarkers of radiation exposure and inflammation stress in human blood. PLoS One. 2012; 7(11):e48619. [PubMed: 23144912]

9. Kim D, Marchetti F, Chen Z, Zaric S, Wilson RJ, Hall DA, et al. Nanosensor dosimetry of mouse blood proteins after exposure to ionizing radiation. Sci Rep. 2013; 3:2234. [PubMed: 23868657]

10. Tucker JD, Joiner MC, Thomas RA, Grever WE, Bakhmutsky MV, Chinkhota CN, et al. Accurate gene expression-based biodosimetry using a minimal set of human gene transcripts. Int J Radiat Oncol Biol Phys. 2014; 88(4):933–9. [PubMed: 24444760]

11. Sproull MT, Camphausen KA, Koblentz GD. Biodosimetry: A Future Tool for Medical Management of Radiological Emergencies. Health Secur. 2017; 15(6):599–610. [PubMed: 29193982]

12. Ghandhi SA, Smilenov LB, Elliston CD, Chowdhury M, Amundson SA. Radiation dose-rate effects on gene expression for human biodosimetry. BMC Med Genomics. 2015; 8:22. [PubMed: 25963628]

13. Langen B, Rudqvist N, Parris TZ, Schuler E, Helou K, Forssell-Aronsson E. Comparative analysis of transcriptional gene regulation indicates similar physiologic response in mouse tissues at low absorbed doses from intravenously administered 211At. J Nucl Med. 2013; 54(6):990–8. [PubMed: 23658216]

14. Paul S, Amundson SA. Development of gene expression signatures for practical radiation biodosimetry. Int J Radiat Oncol Biol Phys. 2008; 71(4):1236–44. [PubMed: 18572087]

15. Schuler E, Parris TZ, Rudqvist N, Helou K, Forssell-Aronsson E. Effects of internal low-dose irradiation from ^{131}I on gene expression in normal tissues in Balb/c mice. EJNMMI Res. 2011; 1(1):29. [PubMed: 22214497]

16. Schuler E, Rudqvist N, Parris TZ, Langen B, Spetz J, Helou K, et al. Time- and dose rate-related effects of internal (177)Lu exposure on gene expression in mouse kidney tissue. Nucl Med Biol. 2014; 41(10):825–32. [PubMed: 25156037]

17. Park WY, Hwang CI, Im CN, Kang MJ, Woo JH, Kim JH, et al. Identification of radiation-specific responses from gene expression profile. Oncogene. 2002; 21(55):8521–8. [PubMed: 12466973]

18. Paul S, Ghandhi SA, Weber W, Doyle-Eisele M, Melo D, Guilmette R, et al. Gene expression response of mice after a single dose of 137CS as an internal emitter. Radiat Res. 2014; 182(4):380–9. [PubMed: 25162453]

19. Abend M, Pfeiffer RM, Ruf C, Hatch M, Bogdanova TI, Tronko MD, et al. Iodine-131 dose dependent gene expression in thyroid cancers and corresponding normal tissues following the Chernobyl accident. PLoS One. 2012; 7(7):e39103. [PubMed: 22848350]

20. Maenhaut C, Detours V, Dom G, Handkiewicz-Junak D, Oczko-Wojciechowska M, Jarzab B. Gene expression profiles for radiation-induced thyroid cancer. Clin Oncol (R Coll Radiol). 2011; 23(4):282–8. [PubMed: 21411301]

21. Ory C, Ugolin N, Schlumberger M, Hofman P, Chevillard S. Discriminating gene expression signature of radiation-induced thyroid tumors after either external exposure or internal contamination. Genes (Basel). 2011; 3(1):19–34. [PubMed: 24704841]

22. Abend M, Badie C, Quintens R, Kriehuber R, Manning G, Macaeva E, et al. Examining radiation-induced in vivo and in vitro gene expression changes of the peripheral blood in different laboratories for biodosimetry purposes: First RENEB gene expression study. Radiat Res. 2016; 185(2):109–23. [PubMed: 26829612]

23. Visweswaran S, Joseph S, Dhanasekaran J, Paneerselvam S, Annalakshmi O, Jose MT, et al. Exposure of patients to low doses of X-radiation during neuro-interventional imaging and procedures: Dose estimation and analysis of gamma-H2AX foci and gene expression in blood lymphocytes. Mutat Res. 2020; 856–857:503237.

24. Visweswaran S, Joseph S, S VH, O A, Jose MT, Perumal V. DNA damage and gene expression changes in patients exposed to low-dose X-radiation during neuro-interventional radiology procedures. Mutat Res. 2019; 844:54–61.

25. DuBois SG, Matthay KK. ^{131}I-Metaiodobenzylguanidine therapy in children with advanced neuroblastoma. Q J Nucl Med Mol Imaging. 2013; 57(1):53–65. [PubMed: 23474635]

26. Sharp SE, Trout AT, Weiss BD, Gelfand MJ. MIBG in neuroblastoma diagnostic imaging and therapy. Radiographics. 2016; 36(1):258–78. [PubMed: 26761540]

27. Campbell K, Karski EE, Olow A, Edmondson DA, Kohlgruber AC, Coleman M, et al. Peripheral blood biomarkers associated with toxicity and treatment characteristics after (131)I-metaiodobenzylguanidine therapy in patients with neuroblastoma. Int J Radiat Oncol Biol Phys. 2017; 99(2):468–75. [PubMed: 28871998]

28. Edmondson DA, Karski EE, Kohlgruber A, Koneru H, Matthay KK, Allen S, et al. Transcript analysis for internal biodosimetry using peripheral blood from neuroblastoma patients treated with (131)I-mIBG, a targeted radionuclide. Radiat Res. 2016; 186(3):235–44. [PubMed: 27556353]

29. DuBois SG, Chesler L, Groshen S, Hawkins R, Goodarzian F, Shimada H, et al. Phase I study of vincristine, irinotecan, and (1)(3)(1)I-metaiodobenzylguanidine for patients with relapsed or refractory neuroblastoma: a new approaches to neuroblastoma therapy trial. Clin Cancer Res. 2012; 18(9):2679–86. [PubMed: 22421195]

30. Amundson SA, Grace MB, McLeland CB, Epperly MW, Yeager A, Zhan Q, et al. Human in vivo radiation-induced biomarkers: gene expression changes in radiotherapy patients. Cancer Res. 2004; 64(18):6368–71. [PubMed: 15374940]

31. Amundson SA, Myers TG, Fornace AJ Jr. Roles for p53 in growth arrest and apoptosis: putting on the brakes after genotoxic stress. Oncogene. 1998; 17(25):3287–99. [PubMed: 9916991]

32. Paul S, Smilenov LB, Amundson SA. Widespread decreased expression of immune function genes in human peripheral blood following radiation exposure. Radiat Res. 2013; 180(6):575–83. [PubMed: 24168352]

33. Wyrobek AJ, Manohar CF, Krishnan VV, Nelson DO, Furtado MR, Bhattacharya MS, et al. Low dose radiation response curves, networks and pathways in human lymphoblastoid cells exposed from 1 to 10cGy of acute gamma radiation. Mutat Res. 2011; 722(2):119–30. [PubMed: 21497671]

34. Rohart F, Gautier B, Singh A, Le Cao KA. mixOmics: An R package for 'omics feature selection and multiple data integration. PLoS Comput Biol. 2017; 13(11):e1005752. [PubMed: 29099853]

35. Lacombe J, Sima C, Amundson SA, Zenhausern F. Candidate gene biodosimetry markers of exposure to external ionizing radiation in human blood: A systematic review. PLoS One. 2018; 13(6):e0198851. [PubMed: 29879226]

36. O'Brien G, Cruz-Garcia L, Majewski M, Grepl J, Abend M, Port M, et al. FDXR is a biomarker of radiation exposure in vivo. Sci Rep-Uk. 2018; 8.

37. Brzoska K, Kruszewski M. Toward the development of transcriptional biodosimetry for the identification of irradiated individuals and assessment of absorbed radiation dose. Radiat Environ Bioph. 2015; 54(3):353–63.

38. Carlin S, Mairs RJ, McCluskey AG, Tweddle DA, Sprigg A, Estlin C, et al. Development of a real-time polymerase chain reaction assay for prediction of the uptake of

meta-[(131)I]iodobenzylguanidine by neuroblastoma tumors. Clin Cancer Res. 2003; 9(9):3338–44. [PubMed: 12960120]

39. Ainsbury EA, Bakhanova E, Barquinero JF, Brai M, Chumak V, Correcher V, et al. Review of retrospective dosimetry techniques for external ionising radiation exposures. Radiat Prot Dosim. 2011; 147(4):573–92.
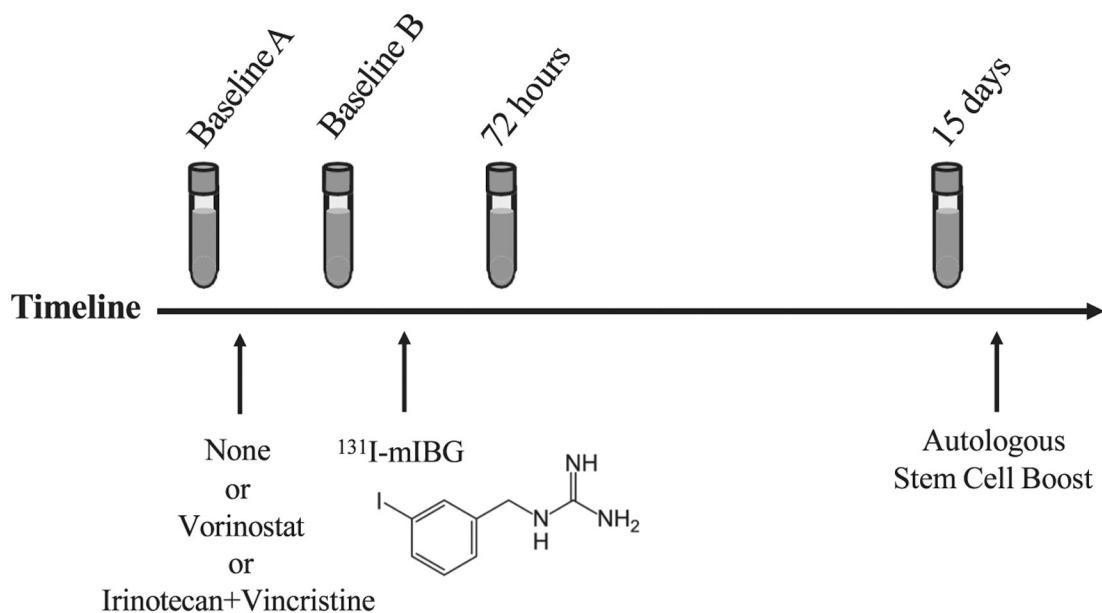
a. Clinical Timeline

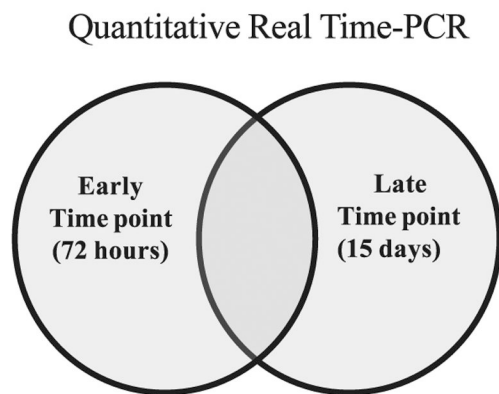## b. Differentially Expressed Transcripts Compared to Untreated Samples

FIG. 1.

Study Design. Panel a: Patients with relapsed or refractory neuroblastoma were treated with ^{131}I-mIBG alone or in combination with vorinostat or irinotecan/vincristine. Blood was drawn prior to any treatment (Baseline A), as well as after introduction of radiation sensitizers (if necessary, Baseline B). All patients were treated with ^{131}I-mIBG, and ^{131}I-mIBG radiotherapy began after blood draw B. Subsequent peripheral blood was drawn at 72 h and day 15 after the start of ^{131}I-mIBG infusion. Panel b: Quantitative real-time PCR was applied to calculate differential transcript expression from the lymphocytes of the
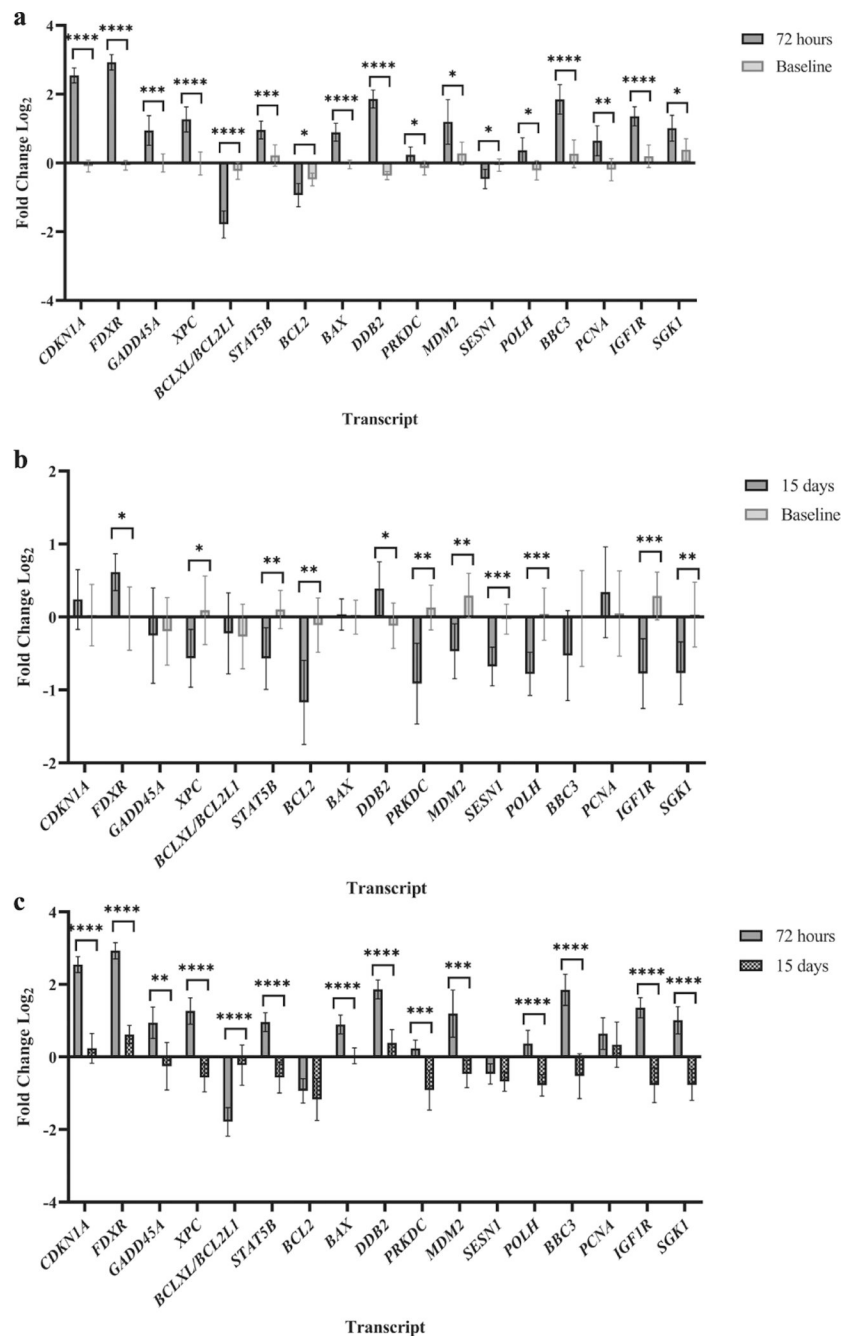
peripheral blood. Differential expression of transcripts was calculated at 72 h and day 15 after ^{131}I-mIBG treatment as compared to untreated controls (Baseline A).

FIG. 2.
Panel a: Differential expression 72 h after ^{131}I-mIBG radiotherapy. Quantitative real-time PCR demonstrates 17 statistically significant transcripts at 72 h after ^{131}I-mIBG treatment. Differential expression from 58 patients and 80 courses of treatment are shown for our top priority transcripts. Shown is the mean $\log_2$ fold change with 95% Confidence Intervals. All fold changes are with respect to untreated blood draw A (Baseline A). Panel b: Differential expression 15 days after ^{131}I-mIBG radiotherapy. Quantitative real-time PCR determined 11 statistically significant transcripts 15 days after ^{131}I-mIBG treatment. *SESN1*, *POLH*, and *IGF1R* displayed the most significant down-regulation from Baseline ($P < 0.001$). Shown

is the mean $\log_2$ fold change with 95% confidence intervals. All fold changes are with respect to untreated blood draw A (Baseline A). Panel c: Observational expression level differences between early and late time points. Quantitative real-time PCR determined fold change fluctuations between early and late time points after[131]I-mIBG treatment. Shown are the mean $\log_2$ fold changes with 95% confidence intervals. All fold changes are with respect to untreated blood draw A (Baseline A).

a.

b.
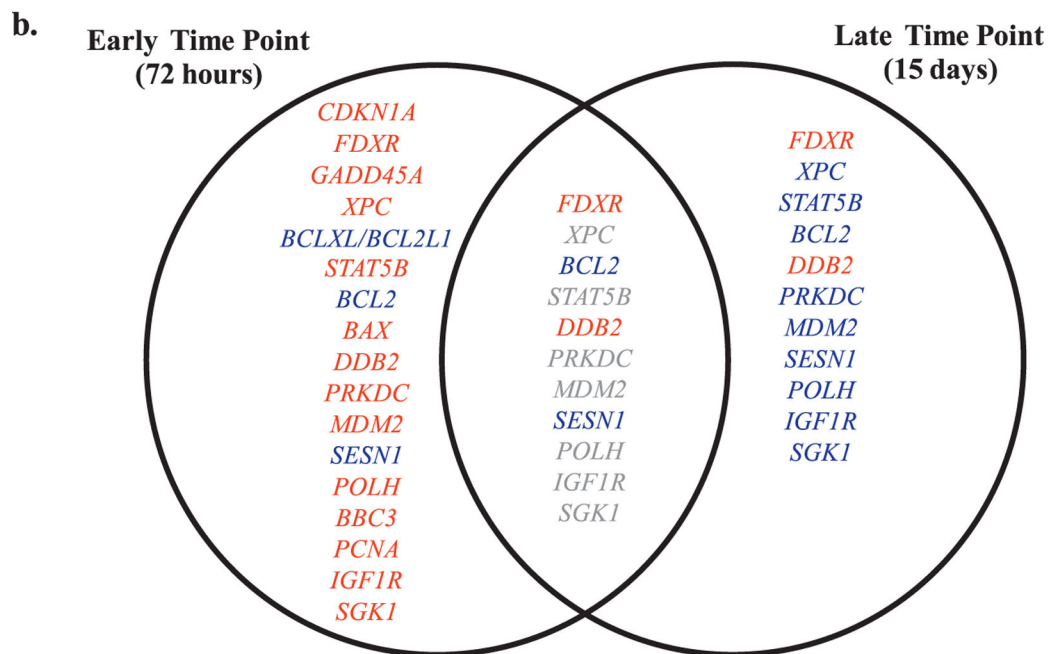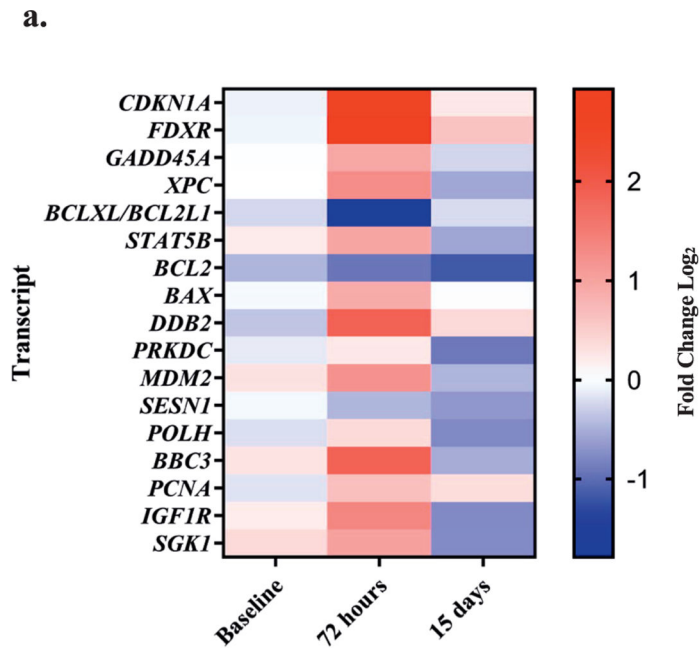
FIG. 3.

Transcripts levels fluctuate between early and late time points. Panel a: Heatmap of average log$_2$ fold changes across time points. Baseline fold change refers to the Baseline B vs. Baseline A comparison. All fold changes are with respect to Baseline A. Panel b: Venn diagram illustrates the differentially expressed transcripts at 72 h, day 15, or the overlap between both time points. Transcript coloring is as follows: up-regulated transcripts (red), down-regulated transcripts (blue), differential expression at both timepoints, but in reverse directions when compared to baseline (gray). All fold changes are log$_2$ transformed and were compared to Baseline A. Differential gene expression cutoff was $P < 0.05$.
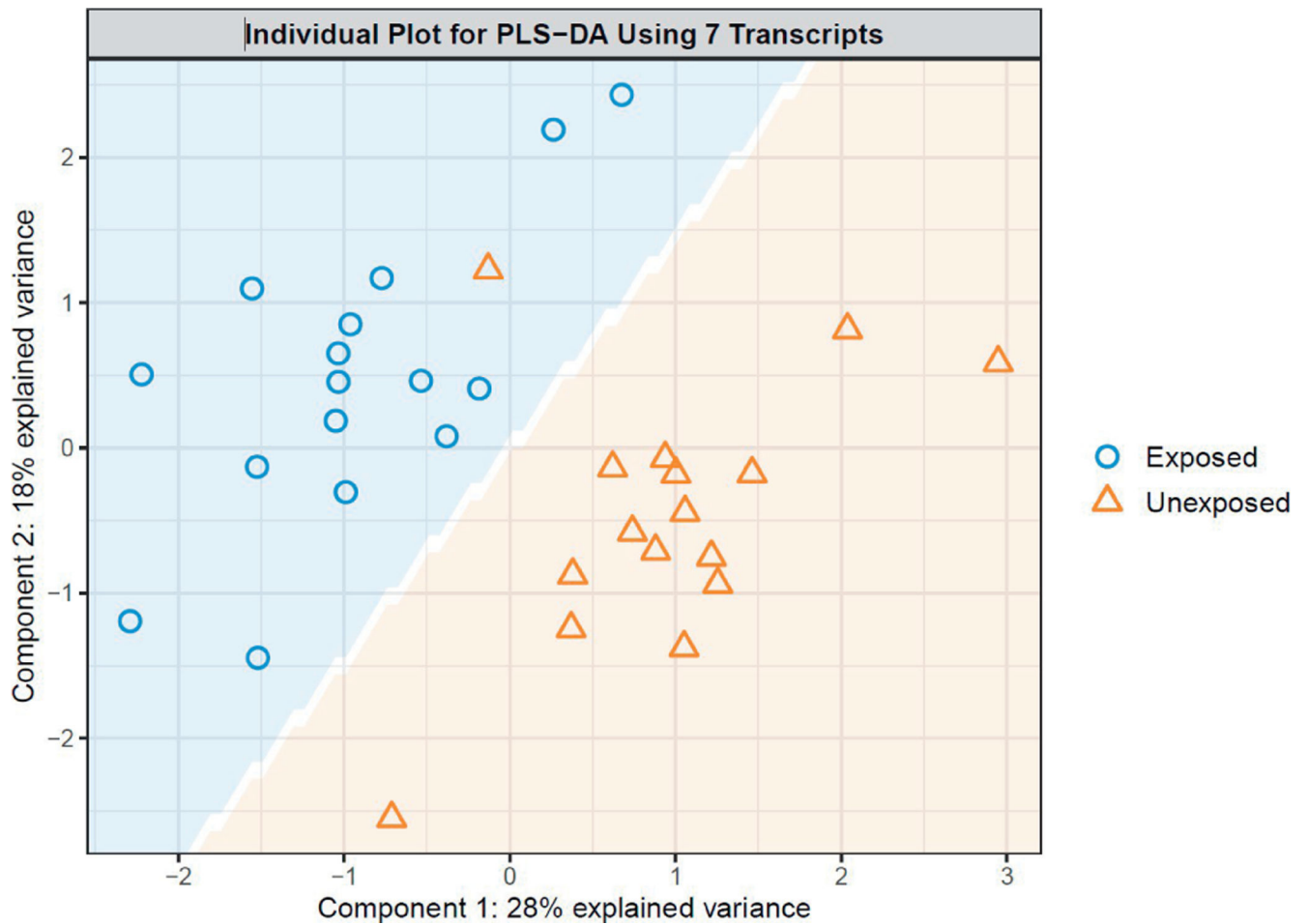
FIG. 4.
Top 7 transcript panel differentiates exposed from non-exposed after 15 days. A predictive two-component PLS-DA model comprised of *CDKN1A*, *FDXR*, *DDB2*, *BCL2*, *BCL2L1*, *DDB2*, and *PRKDC* identified exposed vs. unexposed samples with 87.5% specificity. The color of the background represents the predicted label, and the icons are representative of the actual label.

TABLE 1

Selected Transcripts of Interest

Gene	Name	Primer No.	Pathways	Biological Processes
GAPDH	Glyceraldehyde-3-phosphate dehydrogenase	Hs02758991		Glycolysis
CDKN1A	Cyclin dependent kinase inhibitor 1A	Hs00355782	TP53, ErbB, HIF1, FoxO, PI3K/AKT	DNA damage repair, Cell cycle arrest, apoptosis
FDXR	Ferredoxin reductase	Hs00244586	TP53, Metabolism	Electron transport
BCL2L1/BCLXL	BCL2 like 1	Hs00236329	Ras MAPK, NFKB, TP53, PI3K/AKT	Apoptosis (anti)
BCL2	B-Cell CLL/lymphoma 2	Hs99999018	NFKB, HIF1, TP53, PI3K/AKT	Apoptosis (anti)
BAX	BCL2 associated X protein	Hs99999001	TP53	Apoptosis (pro)
DDB2	Damage specific DNA binding protein 2	Hs03044953	TP53	Nucleotide excision repair
PRKDC	Protein kinase, DNA-activated, catalytic polypeptide	Hs04195439	TP53, PI3K.AKT	DNA repair
GADD45A	Growth arrest and DNA damage inducible alpha	Hs00169255	MAPK, FoxO, TP53, Cell Cycle, p38 JNK	Cell cycle, cellular stress
STAT5B	Signal transducer and activator of transcription 5B	Hs00273500	TCR Signaling	Transcription activator
XPC	Xeroderma pigmentosum, complementation Group C	Hs00190295	TP53	DNA damage repair
BBC3	BCL2 binding component 3	Hs00248075	TP53	Apoptosis (pro)
SESN1	Sestrin 1	Hs00205427	TP53	DNA damage, oxidative stress
POLH	DNA polymerase Eta	Hs00982625	TP53	DNA repair
IGF1R	Insulin-Like growth factor 1 receptor	Hs00181385	PI3K/AKT, Ras MAPK	Tyrosine kinase activity, cell growth and survival, apoptosis (anti)
SGK1	Serum/glucocorticoid regulated kinase 1	Hs00985033	TP53, Ras MAPK	Cellular stress
PCNA	Proliferating cell nuclear antigen	Hs00427214	TP53	DNA repair
MDM2	Mouse double minute 2	Hs00234753	TP53, PI3K/AKT, FoxO	Cell cycle arrest, apoptosis (anti)

TABLE 2

Gene Expression Dose Prediction at 72 h

Patient set	Km dose	GE Dose (Fit)	Lower PI	Upper PI	Lower CI	Upper CI
1	246.25	215.50	113.88	317.13	184.44	246.56
2	283.88	269.84	170.63	369.05	247.95	291.73
3	256.56	261.98	163.21	360.75	242.16	281.80
4	233.92	225.61	126.12	325.11	202.45	248.78
5	251.26	245.56	143.52	347.60	213.18	277.94
6	250.75	155.45	57.19	253.72	138.36	172.55
7	275.89	242.50	144.78	340.21	228.88	256.12
8	254.95	252.93	154.00	351.86	232.36	273.51
9	272.85	237.56	139.65	335.47	222.63	252.49
10	271.75	215.67	117.81	313.52	201.10	230.24
11	259.26	281.64	178.13	385.15	244.89	318.39
12	267.24	254.53	155.60	353.47	233.92	275.14
13	256.56	181.26	83.54	278.98	167.63	194.90
14	275.89	221.45	118.75	324.16	187.04	255.87
15	275.02	257.70	157.67	357.74	232.34	283.07
16	288.13	297.31	197.49	397.13	272.78	321.84
1	0	−32.06	−129.99	65.87	−47.10	−17.02
2	0	10.91	−88.53	110.36	−12.01	33.84
3	0	−24.50	−122.17	73.17	−37.78	−11.21
4	0	−7.15	−110.04	95.73	−42.10	27.80
5	0	6.67	−91.06	104.41	−7.10	20.45
6	0	−66.40	−163.97	31.16	−78.88	−53.92
7	0	−29.87	−127.21	67.47	−40.41	−19.32
8	0	−7.96	−105.11	89.18	−16.51	0.58
9	0	1.77	−95.04	98.57	−1.15	4.68
10	0	−5.00	−102.81	92.81	−19.28	9.28
11	0	28.87	−74.45	132.18	−7.34	65.07
12	0	8.23	−88.83	105.29	0.63	15.84

Patient set	Km dose	GE Dose (Fit)	Lower PI	Upper PI	Lower CI	Upper CI
13	0	−19.41	−116.86	78.03	−30.89	−7.93
14	0	20.43	−77.70	118.55	4.15	36.71
15	0	−7.02	−105.10	91.06	−23.02	8.98
16	0	−11.73	−109.07	85.61	−22.31	−1.16

TABLE 3

LOO-CV at 72 h

	N unexposed	N exposed	AUC	Specificity	Sensitivity
LOO-CV results	80	80	0.9892	0.9875	0.925

Note. Leave one out cross-validation (LOO-CV) on top priority transcripts predicts exposed from unexposed at 72 h.

Author Manuscript

Author Manuscript

Author Manuscript

Author Manuscript

TABLE 4

LOO-CV at Day 15

	N unexposed	N exposed	AUC	Specificity	Sensitivity	
LOO-CV results	16	16	0.8594	0.875	0.875	Top priority transcripts
LOO-CV results	16	16	0.9648	0.9375	0.875	All transcripts

Note. Leave one out cross-validation (LOO-CV) on top priority transcripts predicts exposed from unexposed at day 15.